Intense vortical structures in grid-generated turbulence

E. Villermaux,[a] B. Sixou, and Y. Gagne
LEGI–CNRS, Institut de Mécanique de Grenoble, BP 53X, 38041 Grenoble Cedex, France

(Received 21 December 1994; accepted 11 April 1995)

This paper presents a set of experiments aimed at investigating the features and the statistical frequency of intense vortical structures (sometimes called "filaments", or "worms") as manifested by a migrating bubble technique in a mean shear free, homogeneous, isotropic, stationary turbulence generated by oscillating grids in a water tank for R_λ reaching up to 300. It is found that the nucleation of filaments at the surface of the walls of the tank, where boundary layers are liable to destabilize is much more frequent than in the homogeneous bulk of the tank where one filament is typically detected each hundred large scale turnover time. This distinction between the wall surface and the bulk activity, supplemented with the fact that the size of the filaments and their lifetime compare with the length and time-scales of the largest structures of the flow leads us to formulate an elementary model explaining the origin and the geometrical features of these intense vortical structures in turbulent flows for arbitrary Reynolds numbers. © *1995 American Institute of Physics.*

I. INTRODUCTION AND MOTIVATION

The temptation to reduce a complicated problem characterized by a strong disorder such as three dimensional turbulence to a limited set of simple objects from which one could extract all the statistical quantities of interest is in keeping with a long tradition. Several works have been devoted to the experimental search for well defined and statistically permanent structures in turbulence[1,2] and several authors have examined the consequences of this representation of the flow on its statistical properties such as power spectra, and statistics of velocity increments.[3–8] These works have also been encouraged recently by an increasing number of high resolution numerical simulations showing evidence for the existence in the flow of high vorticity regions organized as elongated filaments.[9–13] Since these filamentary objects, looking like columnar vortices present locally an excess of enstrophy ω^2 compared to their contribution to the dissipation $\varepsilon=\nu\sigma^2$, they also manifest themselves, via the Poisson's law linking the Laplacian of the pressure field to ω^2 and the square of the rate of strain σ^2, as a pressure sink[14–16]: $\nabla^2 P/\rho=\frac{1}{2}[\omega^2-\varepsilon/\nu]$.

Douady *et al.*[15] took advantage of this property and proposed an ingenious experimental technique to visualize these low pressure regions in an experimental configuration close to a circular mixing layer. The technique consists of seeding the medium (water), with small air bubbles which migrate, due to the large density ratio they offer with respect to the ambient fluid, through the pressure gradients towards the depression cores revealing the organization of these cores as transient filamentary objects. These observations were also supplemented by velocity and pressure measurements which showed unambiguously that these filaments are responsible for the deviation from the Gaussian noise of the negative tails in the pressure fluctuation histograms.[17]

However, the flow in this experiment, consisting of two contra-rotating disks in a closed circular vessel, suffers, by construction, from a lack of isotropy at least at large scale since it is dominated by a permanent mean shear and secondary (possibly unstationary) recirculations. This point is significant since most of the observations of these filaments, and all of the pressure measurements in this system (see also Abry *et al.*[18]) are made at the wall of the vessel, and at the position of maximum shear at the midplane between the disks. One might argue that, due to the large value of the Reynolds number usually reached, homogeneity (but not isotropy because of the permanent shear) is recovered at small scale but still the existence and statistical importance of these filaments in a real world experiment independently of any permanent large scale production mechanism (shear) and away from solid boundaries (boundary layer instabilities) remain an open issue. From this remark comes the motivation for the present study.

II. TURBULENCE GENERATED BY OSCILLATING GRID(S)

Mainly used in the context of geophysical applications such as the study of mixing, dispersion in stratified, rotating or two-phase fluids, oscillating grids have drawn interest for their ability to produce a stationary zero mean shear spatially decaying turbulence (Fernando and De Silva[19] and references therein).

A grid (usually square) of mesh size M oscillates around its mean position by an amplitude S (the stroke) at a frequency f in a tank (figure 1). Provided the stroke is not too large compared to M, the frequency not too high and the end conditions of the grid at the walls of the tank are properly realized,[19,20] turbulence away from the grid in the bulk of the tank results form the merging and interaction of the wakes produced by the grid bars during their displacement. The mean velocity of the flow is zero and turbulence decays with increasing distance from the grid to produce, beyond one or two mesh sizes, a flow which is homogeneous in planes parallel to the grid.

If u' denotes the root mean square velocity of $(u'=\langle u(t)^2\rangle^{1/2})$ and L the integral scale of the flow at a distance x from the grid, the spatial evolution laws for the configuration of figure 1a are given by Hopfinger and Toly[20]

[a]E-mail address: villerma@img.fr

 1070-6631/95/7(8)/2008/6/$6.00

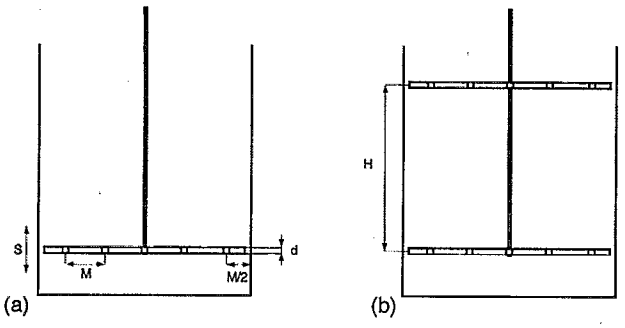

FIG. 1. The two tank configurations used in this study. (a) One grid configuration: The grid is made of fives square bars ($d = 0.8$ cm) spaced by $M = 5.5$ cm in each direction (square mesh). The side bars are spaced by $M/2$ with respect to the walls of the tank. The grid oscillates with a total amplitude $S = 4.5$ cm around its mean position. (b) Two grids configuration: Two identical grids positioned at $H = 5 \times M \approx 28$ cm with respect to each other, respectively on top and at the bottom of the tank are attached to the same central rod and oscillate in phase. A porous ceramic on the floor of the tank through which air was injected allowed to regulate the concentration of bubbles in the tank, containing water, whose temperature could be increased up to 75° Celcius.

$$u' = C_1 f S \frac{(SM)^{1/2}}{x}, \tag{1}$$

$$L = C_2 x. \tag{2}$$

These laws are valid for one grid beyond about one or two mesh sizes away from the grid and for $S \leqslant M$. The coefficients C_1 and C_2 depend on the geometry of the grid. In the present experiments, we used grids of mesh $M = 5.5$ cm, a stroke $S = 4.5$ cm and frequencies f ranging from 3 to 10 Hz. The corresponding coefficients[20] are $C_1 = 0.25$ and $C_2 = 0.2$. Nevertheless, due to the quite fast decrease of u' with x (i.e. $u' \sim 1/x$), the available kinetic energy and therefore the amplitude of the pressure fluctuation (proportional to $\rho u'^2$ if ρ denotes the density of the fluid) vanishes quite rapidly with x.

One is thus tempted to "rectify" the spatial evolution of u' in the center of the box by adding a second grid, identical to the first one, on top of the tank (figure 1b). In our experiment, the two grids are attached to the same central rod, and thus oscillate in phase. They are separated by 5 mesh size M. This separation distance is sufficient to warrant that their wake regions (i.e. $x/M < 1-2$) do not interfere. The central region of the box, close to the midplane between the grids is made more homogeneous with respect to the single grid case, and slightly more intense for the same value of the agitation parameters (M,S and f). Indeed, to understand how the laws (1) and (2) are altered in this new configuration, one has to take into consideration the fact that the energy released in the system per unit time $\varepsilon = u'^2/(L/u') = u'^3/L$ by each grid is *additive*. Thus, at a given location in the box, the local effective dissipation per unit mass ε_{eff} writes

$$\varepsilon_{\text{eff}} = \varepsilon_1 + \varepsilon_2 = \frac{u_1'^3}{L_1} + \frac{u_2'^3}{L_2} \tag{3}$$

where ε_1 and ε_2 are the contributions coming from each grid at that location in the tank.

Close to the central region near the midplane between the grids, the two integral scales L_1 and L_2 are, by symmetry since the two grids are identical, equal. In addition, since the integral scale is only a function of the geometry of the grid, it is, at this intermediate location, also equal to the one given for one grid by (2). Thus $L_1 = L_2 = L$ and it follows from (3), writing ε_{eff} as $u_{\text{eff}}'^3/L$ where u_{eff}' is the effective turbulent velocity with two grids, that

$$u_{\text{eff}}' = 2^{1/3} u' \tag{4}$$

if u' is given by (1) for one grid. This is a slight increase. The main effect using two grids is the confidence that the central region of the box is fairly homogeneous and not biased by a mean decrease. We have concentrated our observations in this region.

Our visualization technique is directly inspired by the one used by the group of Y. Couder (Douady *et al.*,[15] Boon *et al.*,[21] Cadot *et al.*,[17] see also Hopfinger *et al.*[22]). Air bubbles were injected in the tank just below the bottom grid via a porous ceramic producing very small bubbles (approximately 100 μm in size) at a controlled rate, in such a way that the concentration of bubbles could be adjusted at will, independently of the imposed oscillation frequency of the grids. In order to facilitate the migration of the bubbles towards low pressure structures, the medium was heated up to 70°–75° Celcius, thereby reducing its viscosity ($\eta \approx 0.4 \times 10^{-3}$ Pa s and $\rho \approx 970$ kg/m^3 at that temperature). The drag force exerted on a (quasi-spherical) bubble is reduced proportionally to η and the Reynolds number of the flow $\text{Re} = u'L/\nu$ where $\nu = \eta/\rho$ is increased with respect to standard conditions. Throughout all of the configurations, the bulk turbulent Reynolds number $\text{Re} = u'L/\nu$ varied from 1000 to 3000 and the Reynolds number based on the Taylor microscale which writes $R_\lambda = (30\text{Re})^{1/2}$ in grid turbulence when L refers to a transverse integral scale varied from 170 to 300.

III. RESULTS

The visualizations could be carried out according to two distinct operating modes. Either the tank was lit from behind by a white diffuse light, or the center of the box was made visual by a thick sheet of light produced through two slots positioned in front of each other on each side of the tank, perpendicular to the direction of observation (figure 2). In each case the flow was recorded by a CCD camera at a rate of 25 images per second. The first visualization mode (by transmission) offered only a small optical penetration depth in the medium which was rapidly opalescent at working bubble concentrations. This mode was thus appropriate for the observation of the surface activity in the immediate proximity of the wall of the tank (not more than 2 cm in depth).

With the second visualization mode, we were able to concentrate on a region in the bulk of the tank 3×3 cm wide and, according to the width of the slots, 3 cm in depth. At that location from the grids ($x \approx 12.5$ cm), the integral scale L was about 2.5 cm.

These two kind of investigations reveal rather contrasting situations.

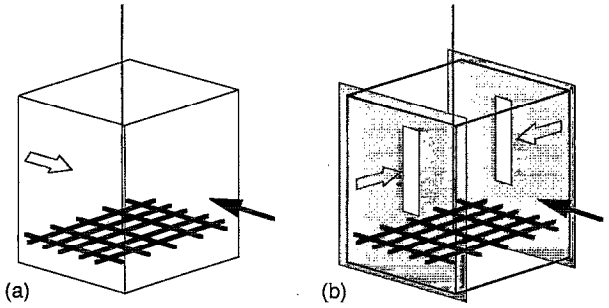

FIG. 2. The two distinct visualization modes. The white arrows indicate the direction of light emission, the black arrows indicate the direction of observation. (a) The tank is lit from behind and, because of the opalescence of the medium due to the presence of bubbles, the optical penetration depth was limited to about 2 cm in the immediate vicinity of the wall. This mode singles out the surface activity. (b) Light is emitted through two slots positioned here and there of the tank, perpendicular to the direction of observation, thus producing a thick ($\approx$3 cm) sheet of light. In both cases, the visualization window was centered at $x \approx 13$ cm from the bottom grid.

A. Near wall activity

The activity of the flow at the walls is permanently sustained by the turbulent motions in the bulk of the tank. It is observed that large eddies impinge periodically at the wall with, most of the time, a preferential direction parallel to the wall, therefore inducing locally a shear that leads if the impingement is sufficiently violent, to a boundary layer instability, enhanced by longitudinal stretch. This mechanism is made visible by the concentration of vorticity in the structures resulting from this primary instability, and thus to the migration of bubbles in the depression cores. These structures show up as elongated dark filaments on a white background, since they correspond to high bubble concentration zones and are illuminated from behind (figure 3). Some of them exhibit a typical pattern of secondary instability in boundary layers, i.e. the evolution towards "lambda" shaped vorticies (figure 3b). The filaments systematically nucleate parallel to the wall, are rather longer than the local bulk integral scale L and can live up to 2 or 3 times the local large scale turnover time $t(L)=L/u'$. Since these surface events are quite frequent, it is possible to compute from a long sequence the statistics of the waiting times Δt between the appearance of two consecutive filaments in the visualization window (figure 4). Normalizing the waiting time Δt by $t(L)$ as $\tau=\Delta t/t(L)$, the probability density function $P(\tau)$ is found to be fairly represented by an exponential decrease $P(\tau)\sim e^{-\alpha\tau}$, with $\alpha\approx 0.5$.

The histograms of waiting times obtained in the configuration of rotating disks[17,18] exhibit also an exponential decay, typical of rare uncorrelated events for intervals τ larger than a few units (the Poisson character of the distribution has been specifically established by Cadot et al.[17]). When replotted in the non-dimensional coordinate $\tau=\Delta t/t(L)$, and assuming $t(L)=2\pi/\Omega$ where Ω is the angular velocity of the discs, the argument α found by Abry *et al.* is of the same order of magnitude as ours ($\alpha\approx 0.3$) weakly varying with the Reynolds number. However, in the circular mixing layer configuration, the primary vortices, originating from the Kelvin–Helmholtz instability of the mean shear profile are as for them perpendicular to the wall (this is also the reason why they are revealed by the pressure measurements at the wall performed by these authors). This numerical coincidence, together with the fact that the average waiting time, but also the mean lifetime of the vortices,[17] scale with the large scale turnover time, could be an indication that these filaments are simply the signature of the existence of a primary instability production mechanism (free shear, boundary layer) in a region of the flow rather than a spontaneous intensification of the vorticity of a smooth turbulent background.

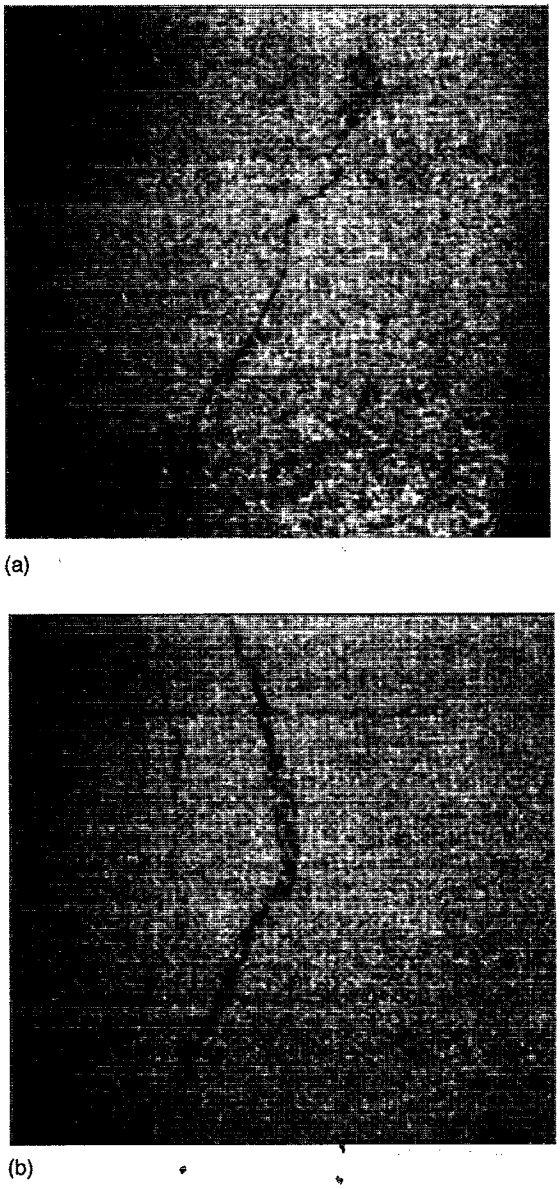

FIG. 3. Surface filaments. The visualization window is 5 cm wide. The filaments, illuminated from behind, appear black on a white background. (a) $\mathrm{Re}=u'L/\nu = 2000$. (b) Same conditions, large scale destabilization in a "lambda" shape, characteristic of boundary layer secondary instability.

B. Bulk filaments

In the center of the box, through a cubic window covering a little bit more than one local integral scale ($3\times3\times3$

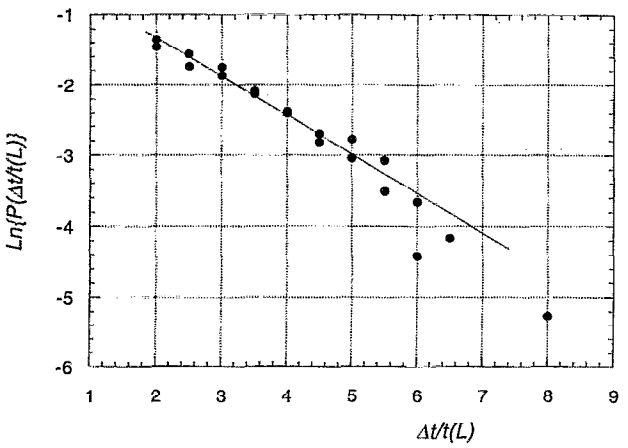

FIG. 4. Histogram of the waiting times between the appearance of consecutive filaments in the visualization window Δt normalized by $t(L)$, for two runs at Re=2200. The scatter among the points gives an idea of the error bars. Setting $\tau=\Delta t/t(L)$. The probability density $P(\tau)$ behaves as $P(\tau)\sim e^{-0.5\tau}$.

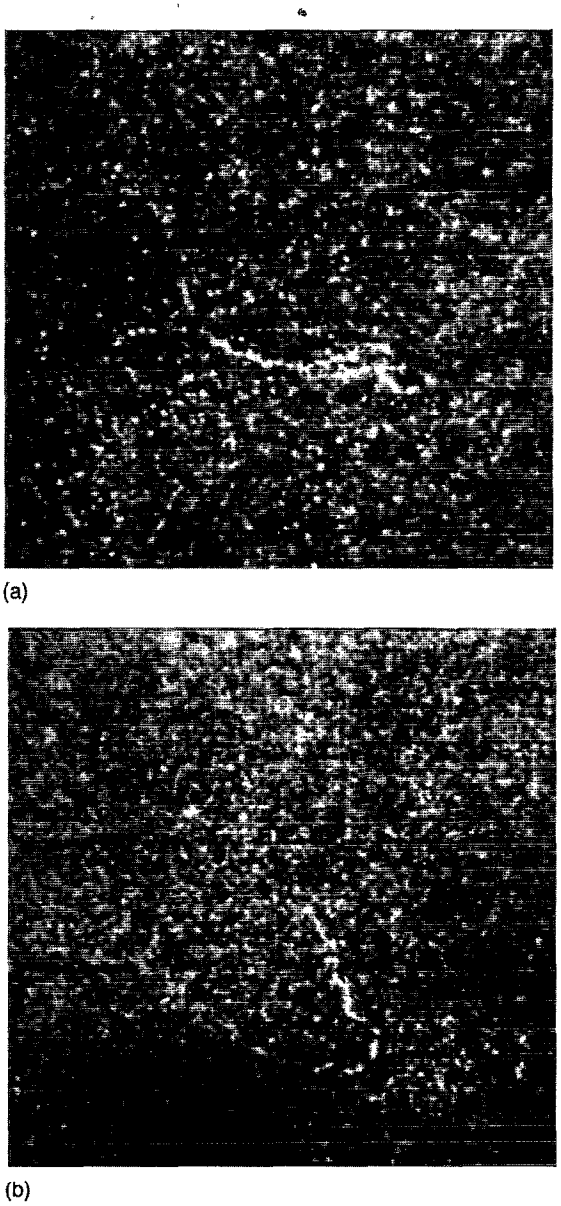

FIG. 5. Bulk filaments. The visualization window is 3 cm wide. The filaments, illuminated from the sides, appear white on a dark background. (a) One grid configuration, Re=1700. (b) Two grid configuration, Re=2200.

cm and $L=2.5$ cm), the flow is characterized by a continuous smooth agitation revealed by smooth spatial fluctuations of the concentration of bubbles. Once in a while however [i.e. once every $100\times t(L)$ approximately], a large scale coherent motion of fluid animated by a strong velocity difference of order u' with respect to its nearby environment precedes the sudden formation of an intense, rapidly distorting and short lived filamentary aggregation of bubbles, showing up as a bright structure on a noisy dark background (in that case the medium is lit from the sides, figures 5a and 5b). The estimation of the magnitude of the velocity difference was made by comparing the position of the bubbles on two successive frames just before the formation of a filament. Considering the framing rate of the camera, the motion of the bubbles was slow enough so that their velocity could be estimated from their displacements by this procedure. The sizes of the filaments are most slightly shorter than L, but no definitive statement is possible because of the perspective effects associated to the random orientation of the filaments. After a complex transient period during which the vortex undergoes either a global bending due to the large scale reorganization of the background flow, or small scale instability of its core (wiggles), or both, the vortex disappears abruptly. Rarely are secondary or subsequent smaller filaments detected. The lifetime of the bulk filament is found to scale with the integral scale turnover time $t(L)=L/u'$ and represents roughly a quarter of this time scale, irrespectively of the turbulent Reynolds number for $1000<\mathrm{Re}<3000$ (figure 6). We would like to emphasize at this point that, within this crude experimental visualization technique of migrating bubbles, these objects in the bulk are detected as rare events (at least compared to the surface ones) and that they seem to be attached, in lengthscale and timescale, to the dynamics of the largest structures of the flow.

Needless to say, invoking Plato's Cavern Allegory, we are aware that our observations are probably very sensitive to and dependent on the visualization technique used. This technique definitely filters only the strongest events, that is the filaments with a large peripheral velocity. If we estimate the peripheral velocity of the filaments we observe by u' (see section IV and also Cadot *et al.*[17]) and the viscous radius of the vortices as several units of the Kolmogorov scale (a lengthscale which compares to the diameter of the bubbles), the migration time t_m required for a bubble to reach the viscous core of the vortex starting from an initial position, say, twice the vortex radius is provided by the balance of acceleration seen by the bubble $(\pi d^3/8)\ (\Delta\rho/\rho)\ (\mathrm{d}P/\mathrm{d}r)$ in the radial pressure gradient $\mathrm{d}P/\mathrm{d}r=\rho\Gamma^2/4\pi^2r^3$ and the viscous drag for small air bubbles[23] $-3\pi d\eta\ (\mathrm{d}r/\mathrm{d}t)$, if ρ denotes the density of water, $\Delta\rho\approx\rho$ the difference of density between water and air, and Γ the circulation of the vortex. It is found that $t_m\approx 70\nu/u'^2$. With $u'\approx 3\times10^{-2}$ m/s and $\nu\approx 0.4\times10^{-6}$ m^2/s, the migration time t_m is estimated to be of the order of 0.03 s, a time that compares to the inverse of

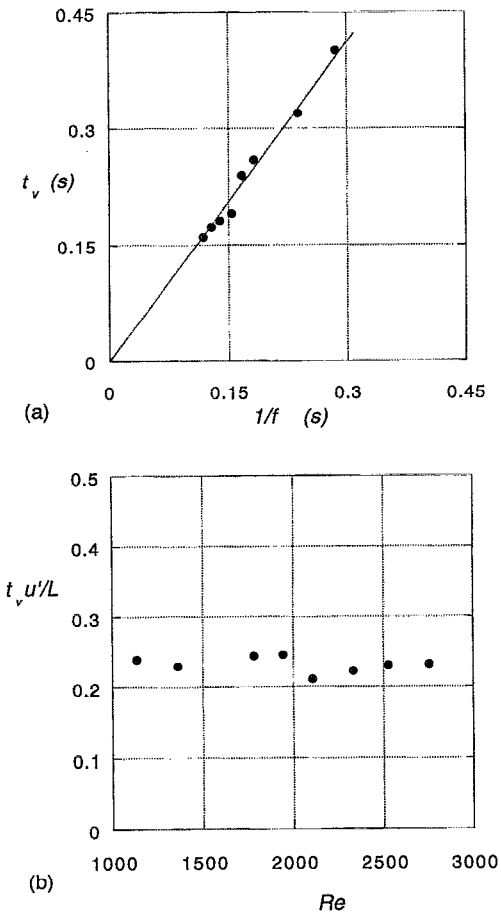

FIG. 6. Lifetime t_v of the bulk filaments. (a) t_v versus $1/f$, where f is the oscillation frequency of the grid. (b) Lifetime rescaled by the large scale turnover time $t(L)=L/u'$ as a function of Re.

the framing rate of the camera (we indeed observe the formation of the filaments on a duration that does not exceed 1/50 s). It is clear that, for a filament to be clearly identified as such, the separation between its formation time, typically given by t_m, and its lifetime, typically given by $0.25\times t(L)$, has to be large. This simple effect naturally selects the filaments associated with vortical structures pertaining to the large scales.

But we do emphasize, as well, that we observe only these large scale filaments. This leads us to some elementary considerations about their origin and their formation.

IV. DISCUSSION

We have already mentioned that the formation of a filament in the bulk was preceded by a large scale coherent motion of fluid at the same location in the flow. This finding provides us with a possible scenario for the origin of these events: suppose that a packet of fluid of typical size L happens, intermittently, to present a motion of solid translation with respect to its environment, with a velocity of order u'. We set aside for the moment the estimation of the probability of this event. This motion will, most probably, last for a time $t(L)$ corresponding to the displacement time of the packet by a distance of its own size L, that is $t(L)\sim L/u'$.

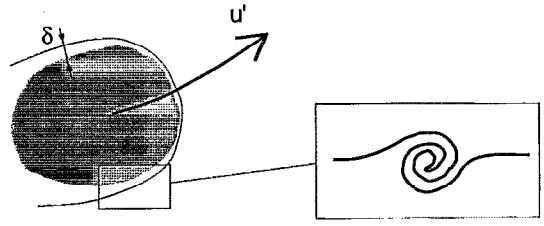

FIG. 7. Sketch of a possible scenario for the formation of intense vortical structures in turbulence. A velocity difference of order u' is intermittently established over a scale $\delta\sim\sqrt{\nu L/u'}$. Provided the Reynolds number $\mathrm{Re}_\delta=u'\delta/\nu$ is large enough (>100 typically), this shear layer destabilizes through a Kelvin–Helmholtz process to form a concentrated vortex of radius of order δ and of circulation $\Gamma\sim u'\delta$. The probability of occurrence of this scenario is, away from any permanent vorticity production mechanism (wall, permanent shear) of order $\frac{1}{8}e^{-0.7\mathrm{Re}^{1/6}}$ with $\mathrm{Re}=u'L/\nu$.

Subsequent to this relative motion, a diffusive shear layer forms around the packet (figure 7), whose thickness δ scales as

$$\delta\sim\sqrt{\frac{\nu L}{u'}}. \tag{5}$$

Note that at this level of description of the phenomenon, the thickness δ according to the above qualitative scenario is identical to an expression such that $\delta\sim\sqrt{\nu/\gamma}$ involving a large scale spanwise strain rate $\gamma=u'/L$ so that both interpretations may be valid. Now, this shear layer, experiencing a velocity difference u' on a width δ will, provided the Reynolds number $\mathrm{Re}_\delta=u'\delta/\nu$ is sufficiently large, destabilize via a classical Kelvin–Helmholtz process to form a roll-up vortex. The length of the vortex just after this primary instability corresponds to the spanwise extent of the support of the shear layer, that is L, and the size of its viscous core is of order δ; this object therefore shows up as a large aspect ratio filamentary structure of circulation $\Gamma\sim 2\pi u'\delta$. This model is particularly sensitive to two points that might serve to test it.

First, the growth rate of the Kelvin–Helmholtz instability of a shear layer whose thickness is controlled by diffusion is known to be strongly affected (i.e. damped) as soon as the Reynolds number Re_δ is lower than about 150 (Betchov and Szewczyk[24]). Note that Re_δ is proportional to the square root of the turbulent Reynolds number $\mathrm{Re}=u'L/\nu$ and thus scales as R_λ. The present experiments, with $170<R_\lambda<300$, have been performed just above this threshold and we also have to mention that no filament could be detected any more below $\mathrm{Re}=1000$ ($R_\lambda=170$). This would suggest that a critical turbulent Reynolds number has to be reached, corresponding to a critical microscopic Reynolds number Re_δ (or, equivalently, R_λ) for these filaments to be able to nucleate in the medium, the effect of viscosity being predominant below. This phenomenon could suggest that the structure of turbulence undergoes a continuous (second order) critical transition above R_λ about a few hundreds[25] simply because of the damping action of viscosity on a Kelvin–Helmholtz instability, first and necessary step of the formation of filamentary concentrated vortices linking large to small scales, whose breakdown could be a *sine qua non*

condition for the existence of an inertial range. This suggestion has to be moderated by the fact that the intense filaments are detected as rare events when in that case at least one filament per integral scale cubic volume L^3 and per turnover time $t(L)$ should be requested. This point could also be advantageously clarified by numerical simulations.[26]

Second, we have up to now said nothing about the probability of realization of our scenario, which is essentially the probability of existence in the flow of a velocity difference of order of the large scale excursion u' over a distance δ controlled by diffusion effects, scaling like the Taylor microscale λ as a function of Re [see equation (5)]. The PDF of velocity differences over such distances in the dissipative range ($r/\eta<30$) are known to be broad, with exponential tails; if σ denotes the root mean square value of the velocity difference over a distance δ, then the probability density to find a velocity difference of modulus u over this distance is given approximately, at Reynolds numbers R_λ about a few hundreds, by[27]

$$P\left(\frac{u}{\sigma}\right)\approx \frac{b}{8\sigma}\, e^{-b\frac{u}{\sigma}} \text{ with } b\approx 0.7, \tag{6}$$

this expression being a fit of the PDF valid for $u\geqslant 3\sigma$. (See also the simulations of Vincent and Meneguzzi[10] whose PDF's fit precisely to this form at a similar Reynolds number.) Let σ be computed by the Kolmogorov estimate $\sigma=u'(\delta/L)^{1/3}$; we see that our problem amounts to estimate the probability p for the velocity increment u to be of the order of the large scale excursion u' or more, across the separation distance δ. Since the PDF is a rapidly decreasing function of u, the probability p is dominated by the lower bound of the integral

$$p\approx \int_{u'}^{\infty} P\left(\frac{u}{\sigma}\right) du, \tag{7}$$

that is $p\approx \frac{1}{8}\, e^{-b(u'/\sigma)}$. With $\delta\sim(\nu L/u')^{1/2}$, this probability is therefore $p\approx \frac{1}{8}\, e^{-0.7\mathrm{Re}^{1/6}}\approx 0.013$ at $\mathrm{Re}=1000$ and $p\approx 0.008$ at $\mathrm{Re}=3000$, in good agreement with our observations: assuming that such an event is followed by the formation of a filament, the probability to observe a filament during a period of observation $t(L)$ in a box covering a cubic integral scale L^3 should be, according to the above reasoning, of order 1/100, and we indeed find that the appearance of a filament in the bulk occurs, in the mean, each 100 large scale turnover time $t(L)$.

It is clear that in the regions of the flow where our scenario is forced to occur most of the time, that is in the vicinity of a wall developing unstable boundary layers, or in an externally maintained shear, the probability of this favorable event for the formation of a filament becomes order unity [one filament per turnover time $t(L)$], as suggested by our, and other authors observations.[15,17]

ACKNOWLEDGMENTS

We acknowledge O. Cadot, Y. Couder and S. Douady for the interest they manifested in this experiment and for their comments. Discussions with E. J. Hopfinger, E. Gledzer and A. Pumir have also been useful. E. Villermaux wishes to thank the Centre Emile Borel of the Institut Henri Poincaré, where part of this paper was written, for its hospitality.

[1] G. K. Batchelor and A. A. Townsend, "The nature of turbulent motion at large wave-number," Proc. R. Soc. London Ser. A **199**, 238 (1949).
[2] A. Y. S. Kuo and S. Corrsin, "Experiments on internal intermittency and fine-structure distribution functions in fully turbulent fluid," J. Fluid Mech. **50**, 285 (1971).
[3] A. A. Townsend, "On the fine scale structure of turbulence," Proc. R. Soc. London Ser. A **208**, 534 (1951).
[4] H. K. Moffat, S. Kida, and K. Ohkitani, "Stretched vortices–the sinews of turbulence; large-Reynolds-number asymptotics," J. Fluid Mech. **259**, 241 (1994).
[5] A. D. Gilbert, "A cascade interpretation of Lundgren's stretched spiral vortex model for turbulent fine structure," Phys. Fluids A **5**, 2831 (1993).
[6] J. C. Vassilicos, "The multispiral model of turbulence and intermittency," in *Topological Aspects of the Dynamics of Fluids and Plasmas*, edited by H. K. Moffatt, G. M. Zaslavsky, P. Comte, and M. Tabor (Kluwer Academic, New York, 1992), p. 427
[7] Z. S. She and E. Leveque, "Universal scaling laws in fully developed turbulence," Phys. Rev. Lett. **72**, 336 (1994).
[8] H. Tennekes, "Simple model for the small-scale structure of turbulence," Phys. Fluids **11**, 669 (1968).
[9] E. D. Siggia, "Numerical study of small scale intermittency in three dimensional turbulence," J. Fluid Mech. **107**, 375 (1981).
[10] A. Vincent and M. Meneguzzi, "The spatial structure and statistical properties of homogeneous turbulence," J. Fluid Mech. **225**, 1 (1991).
[11] A. Vincent and M. Meneguzzi, "The dynamics of vorticity tubes in homogeneous turbulence," J. Fluid Mech. **258**, 245 (1994).
[12] J. Jiménez, A. A. Wray, P. G. Saffman, and R. S. Rogallo, "The structure of intense vorticity in isotropic turbulence," J. Fluid Mech. **255**, 65 (1993).
[13] O. Métais and M. Lesieur, "Spectral large eddy simulation of isotropic and stably-stratified turbulence," J. Fluid Mech. **239**, 157 (1992).
[14] M. E. Brachet, "Géométrie des structures à petite échelle dans le vortex de Taylor–Green," C. R. Acad. Sci. Paris **311**, (II), 775 (1990).
[15] S. Douady, Y. Couder, and M. E. Brachet, "Direct observation of the intermittency of intense vorticity filaments in turbulence," Phys. Rev. Lett. **67**, 983 (1991).
[16] A. Pumir, "A numerical study of pressure fluctuations in three-dimensional, incompressible, homogeneous, isotropic turbulence," Phys. Fluids **6**, 2071 (1994).
[17] O. Cadot, S. Douady, and Y. Couder, "Characterization of the low pressure filaments in a 3D turbulent shear flow," Phys. Fluids **7**, 630 (1995).
[18] P. Abry, S. Fauve, P. Flandrin, and C. Laroche, "Analysis of pressure fluctuations in swirling turbulent flows," J. Phys. II France **4**, 725 (1994).
[19] H. J. S. Fernando and I. P. D. De Silva, "Note on secondary flows in oscillating-grid, mixing box experiments," Phys. Fluids A **5**, 1849 (1993).
[20] E. J. Hopfinger and J. A. Toly, "Spatially decaying turbulence and its relation to mixing across density interfaces," J. Fluid Mech. **78**, 155 (1976).
[21] D. Bonn, Y. Couder, P. H. J. van Dam, and S. Douady, "From small scales to large scales in three-dimensional turbulence: the effect of diluted polymers," Phys. Rev. E **47**, R28 (1993).
[22] E. J. Hopfinger, F. K. Browand, and Y. Gagne, "Turbulence and waves in a rotating tank," J. Fluid Mech. **125**, 505 (1982).
[23] G. K. Batchelor, *An Introduction to Fluid Dynamics* (Cambridge University Press, Cambridge, 1967).
[24] R. Betchov and G. Szewczyk, "Stability of a shear layer between parallel streams," Phys. Fluids **6**, 1391 (1963).
[25] B. Chabaud, A. Naert, J. Peinke, F. Chillà, B. Castaing, and B. Hébral, "A transition toward developed turbulence," Phys. Rev. Lett. **73**, 3327 (1994).
[26] M. E. Brachet, M. Meneguzzi, A. Vincent, H. Politano, and P. L. Sulem, "Numerical evidence of smooth self-similar dynamics and possibility of subsequent collapse for three-dimensional ideal flows," Phys. Fluids A **4**, 2845 (1992).
[27] Y. Gagne, Ph.D. thesis, Institut National Polytechnique de Grenoble, 1987; Y. Gagne, E. J. Hopfinger, and U. Fisch, "A new universal scaling for fully developed turbulence: the distribution of velocity increments," in *New Trends in Nonlinear Dynamics and Pattern-Forming Phenomena*, edited by P. Coullet and P. Huerre (Plenum, New York, 1990).